

New Physics Beyond the Standard Model at $\gamma\gamma$ Colliders ¹

Thomas G. Rizzo ^a

^a*Stanford Linear Accelerator Center, Stanford CA 94309, USA*

Abstract

The complementarity of e^+e^- and $\gamma\gamma$ colliders to discover and explore new physics beyond the Standard Model(SM) is discussed. After briefly surveying a number of various new physics scenarios we concentrate in detail on signatures for Large Extra Dimensions via the process $\gamma\gamma \rightarrow WW$.

1 Introduction

As is well known there are two ways in which new physics beyond the SM may manifest itself. In the direct scenario, a new particle (or set of particles) may be singly or pair produced at a collider. In the indirect scenario, precision measurements would determine at a high level of confidence that deviations from the SM are found for a particular observable or set of observables. This set of deviations may or may not be sufficient in their magnitude or direction to point to the correct new physics scenario from which they arose.

In the case of direct production it is important to note that the cross sections for pairs of scalars, fermions or vectors particles are all significantly larger at $\gamma\gamma$ colliders than they are at e^+e^- colliders (even after angular acceptance cuts) with comparable luminosities anticipated at both machines. However, by comparison, the $\gamma\gamma$ search reach is reduced due to the high energy cutoff in the

¹ Work supported by the Department of Energy, Contract DE-AC03-76SF00515

photon fluxes. While polarized $\gamma\gamma$ colliders allow one to isolate the couplings of new physics to photons and probe spin configurations not accessible in e^+e^- collisions, they cannot produce neutral particles except via loops, though such cross sections may in some cases be large. For indirect searches both polarized e^+e^- and $\gamma\gamma$ colliders lead to a similar number of final states which have somewhat comparable statistical power as far as looking for deviations are concerned. However, in some cases the $\gamma\gamma$ collider has the edge due to the larger cross sections. Based on these arguments alone, and not knowing the source of new physics *a priori*, we would expect a general complementarity for e^+e^- and $\gamma\gamma$ for new physics searches. Unfortunately, analyses of new physics scenarios are not yet as evolved in $\gamma\gamma$ collisions as they are for e^+e^- .

2 Some Examples

There are a number of examples of new physics scenarios which clearly display this complementarity. Perhaps the most well known amongst these possibilities are the anomalous gauge couplings of the W and searches for leptoquarks. While there have been extensive analyses(1) of anomalous triple gauge boson couplings at e^+e^- colliders, the corresponding processes $\gamma e \rightarrow W\nu$ and $\gamma\gamma \rightarrow WW$ have generally gotten less attention in the literature(2). Note that while $\gamma e \rightarrow W\nu$ and $\gamma\gamma \rightarrow WW$ isolate the anomalous photon couplings to the W , $e^+e^- \rightarrow WW$ also potentially involves anomalous Z couplings which may also be present. This process is also dominated by the large t -channel neutrino exchange diagram which can be removed using beam polarization. Perhaps the best example of this complementarity is displayed in the study of Choi and Shrempp that compares the sensitivities of these three processes to the anomalous couplings $\Delta\kappa_\gamma = 1 - \kappa_\gamma$ and λ_γ which is shown in Fig.1. Though now outdated, one sees from this analysis that the sensitivities of the three experiments are qualitatively similar and their overlapping region is substantially smaller than that obtained from any single measurement. It would be very interesting, and perhaps quite important, to repeat this analysis using modern luminosities which are more than an order of magnitude larger than used in this study and to include the increased set of observables that can be used to constrain these anomalous couplings. It is easy to imagine that the resulting area of overlap would now be smaller by more than two orders of magnitude. In the case of anomalous quartic gauge couplings, they can be probed at $\gamma\gamma$ colliders through processes which occur at order α^2 whereas they can only be accessed in e^+e^- collisions at order α^3 giving a great advantage to $\gamma\gamma$ colliders.

Leptoquarks(3) have been well studied in e^+e^- , γe and $\gamma\gamma$ colliders. Buchmüller, Rückl and Wyler have long ago shown that under reasonably general assump-

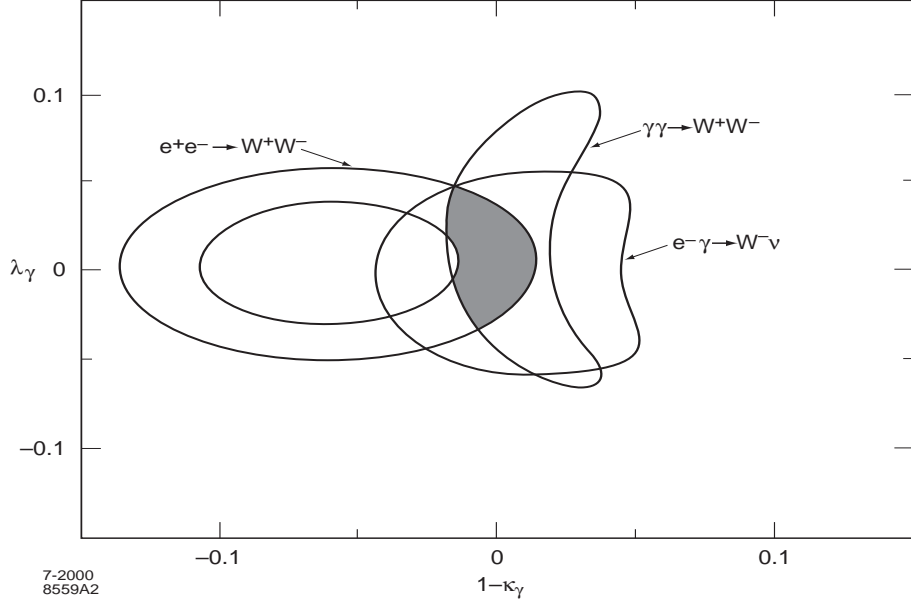


Fig. 1. Allowed overlapping regions from the analysis of Choi and Schrempp in the $\Delta\kappa_\gamma - \lambda_\gamma$ anomalous coupling plane.

tions leptoquarks can arise in any of 14 different varieties. Leptoquarks may have fermion number $F = 0, \pm 2$, come in singlets, doublets or triplets of weak isospin and are either scalars or vectors. (There may even be some evidence for the existence of leptoquarks in the mass range near 400 GeV(4).) Since the LHC will run before any high energy e^+e^- or $\gamma\gamma$ collider and discover(or not) any leptoquarks in the mass range accessible to these machines, their true role is not leptoquark discovery but leptoquark *identification*. Assuming these particles are elementary, a given leptoquark species is easily identified in e^+e^- collisions through the energy dependence of it's total cross section and angular distribution. However, if form factors are present and/or leptoquarks have gauge strength Yukawa couplings it is possible that confusion can arise and a polarized $\gamma\gamma$ collider will be needed to disentangle the various ID possibilities. Since leptoquark charges, Q , vary in magnitude between $1/3$ and $5/3$ and their production cross sections at $\gamma\gamma$ are proportional to Q^4 , a wide range of rates can be expected. This is shown explicitly in Fig.2 from (5) for a $\sqrt{s}=1$ TeV collider.

Note that similar complementarity between e^+e^- and $\gamma\gamma$ colliders also arises in the case of excited fermion production(6).

3 $\gamma\gamma \rightarrow WW$ in Theories with Large Extra Dimensions

In theories with large extra dimensions(7) the exchange of Kaluza-Klein(KK) graviton towers result in large set of new dimension-8 operators that can

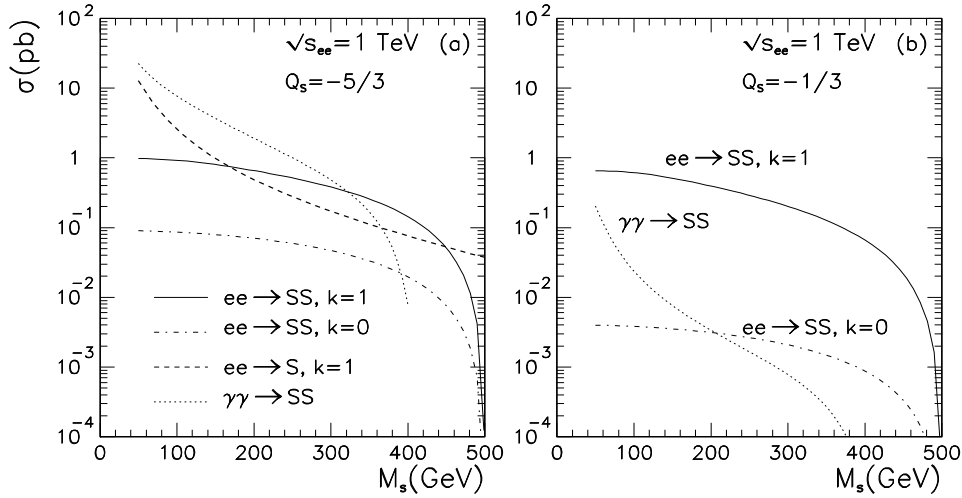


Fig. 2. LQ pair-production cross sections at e^+e^- and $\gamma\gamma$ colliders. Here k is the Yukawa coupling strength in units of strength of e for t - or u -channel quark exchange graphs. Cross sections are shown for the two extreme charge cases of $Q = 5/3$ and $Q = -1/3$.

lead to new contributions to the matrix elements for a number of different processes(8). These exchanges can cause substantial deviations in cross sections, angular distributions and asymmetries. These operators in principle have an arbitrary sign, $\lambda = \pm 1$, and an associated cutoff mass scale, M_H , which is of order the higher dimensional Planck scale. Of the many processes examined so far, $\gamma\gamma \rightarrow WW$ provides the greatest reach for M_H in comparison to the overall collider center of mass energy. (It is difficult to compare the \sqrt{s} dependence of this reach for hadron colliders and $e^+e^-/\gamma\gamma$ colliders.) The main reasons for this are that the WW final state offers many observables which are particularly sensitive to the initial electron and laser polarizations as well as the very high statistics available (due to the 80 pb cross section) with which to probe graviton KK contributions. The differential cross sections are shown in Fig.3 for the SM as well as when the KK tower is included for $\lambda = 1$.

Note that within the SM there is no dramatically strong sensitivity to the initial state lepton and laser polarizations and all of the curves have roughly the same shape. When the graviton tower contributions are included there are several effects. First, all of differential distributions become somewhat more shallow at large scattering angles but there is little change in the forward and backward directions due to the dominance of the SM poles. Second, there is now a clear and distinct sensitivity to the initial state polarization selections. In some cases, particularly for the $(-++-)$ and $(+-+-)$ helicity choices, the differential cross section increases significantly for angles near 90° taking on an m-like shape. This shape is, in fact, symptomatic of the spin-2 nature of the

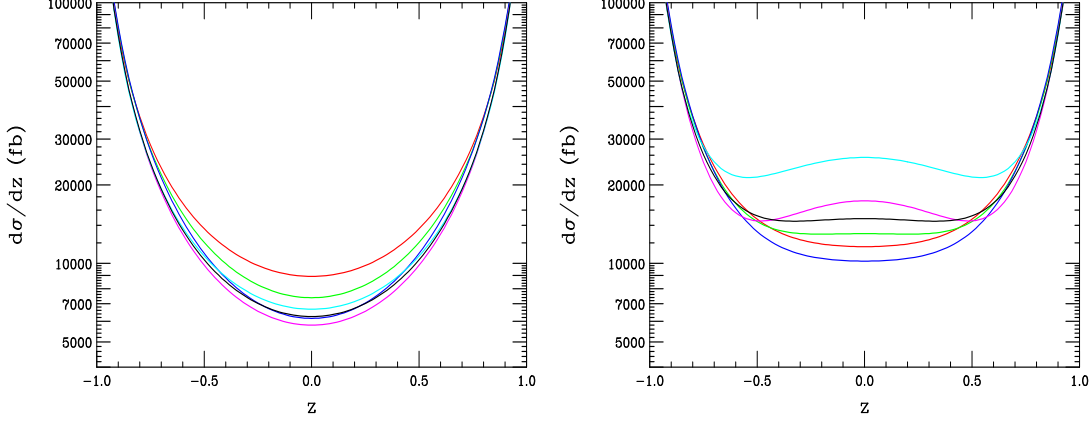


Fig. 3. Differential cross section for $\gamma\gamma \rightarrow W^+W^-$ at a 1 TeV e^+e^- collider for (left) the SM and with $M_H = 2.5$ TeV with (right) $\lambda = 1$. The $\lambda = -1$ results are quite similar. In (left) from top to bottom in the center of the figure the helicities are $(+++)$, $(+++-)$, $(-+-)$, $(+--)$, $(+---$), and $(+--+)$; in (right) they are $(-+-)$, $(+--)$, $(+++-)$, $(+---$), $(+++)$, and $(+--+)$, where we have employed the notation $(P_{e1}, P_{l1}, P_{e2}, P_{l2})$.

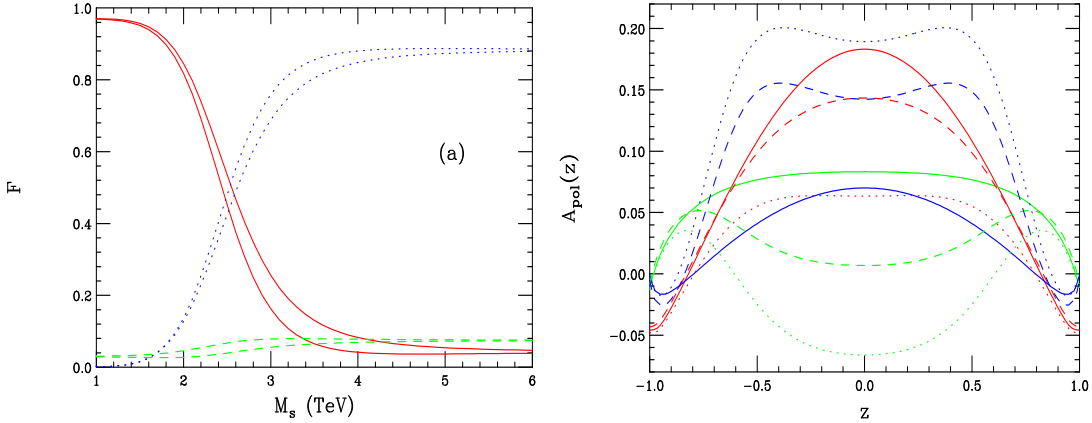


Fig. 4. (Left) Fraction of LL (solid), TL+LT (dashed) and TT (dotted) W^+W^- final states after angular cuts for the process $\gamma\gamma \rightarrow W^+W^-$ at a 1 TeV e^+e^- collider as a function of M_H for either sign of λ . The initial state polarization is $(-+-)$. (Right) Differential polarization asymmetries for $\gamma\gamma \rightarrow W^+W^-$ at a 1 TeV e^+e^- collider for the SM (solid) as well with graviton tower exchange with $M_H = 2.5$ TeV with $\lambda = \pm 1$ (the dotted and dashed curves). We label the three cases shown by the first entry in the numerator in the definition of A_{pol} . Red curves (from top to bottom being the 2nd, 4th and 7th) represent an initial polarization of $(+++)$, green is for the choice $(+++-)$ (the 1st, 3rd and 5th curves) and blue is for the case $(-+-)$, (the 6th, 8th and 9th curves).

K-K graviton tower exchange since a spin-0 exchange leads only to a flattened distribution. Given the very large statistics available with a typical integrated luminosity of $100-300 \text{ fb}^{-1}$, it is clear that the $\gamma\gamma \rightarrow W^+W^-$ differential cross section is quite sensitive to M_H especially for the two initial state helicities specified above.

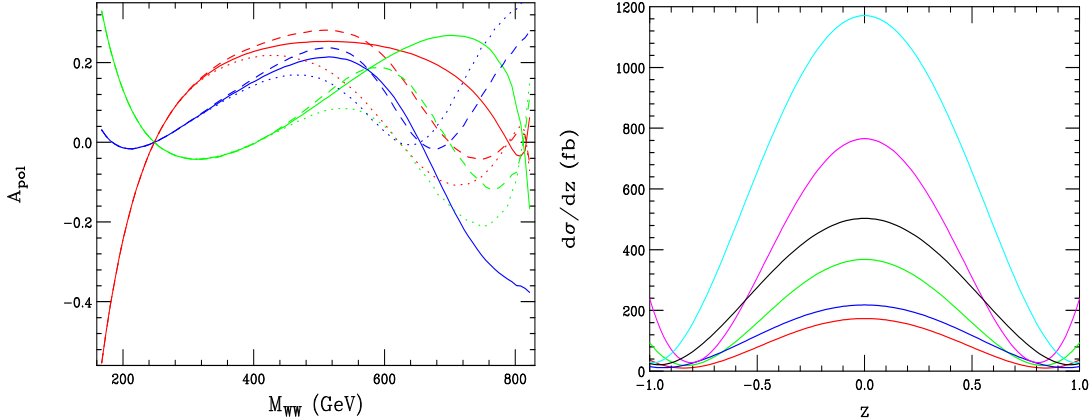


Fig. 5. (Left) Integrated polarization asymmetries for $\gamma\gamma \rightarrow W^+W^-$ at a 1 TeV e^+e^- collider as functions of the WW invariant mass. The labels for the various curves are as in the previous figure and a cut of $|z| < 0.8$ has been applied. (Right) Differential cross section for $\gamma\gamma \rightarrow ZZ$ at a 1 TeV e^+e^- collider due to the exchange of a K-K tower of gravitons assuming $M_H = 3$ TeV. From top to bottom in the center of the figure the initial state helicities are $(- + +-)$, $(+ - +-)$, $(+ - --)$, $(+ + +-)$, $(+ + --)$, $(+ + ++)$.

In the SM, the final state W 's are dominantly transversely polarized. Due to the nature of the spin-2 graviton exchange, the K-K tower leads to a final state where both W 's are instead completely longitudinally polarized. This is shown explicitly in Fig.4 where we see the fraction of longitudinally polarized W 's falling rapidly as the scale M_H is increased in comparison to \sqrt{s} . Thus we might expect that a measurement of the W polarization will be a sensitive probe M_H . Other observables can be constructed out of the polarization dependent cross sections themselves. For the six possible initial state polarizations one can construct three independent polarization asymmetries of the form

$$A_{pol}(z) = \frac{d\sigma(P_{e1}, P_{l1}, P_{e2}, P_{l2}) - d\sigma(P_{e1}, P_{l1}, -P_{e2}, -P_{l2})}{d\sigma(P_{e1}, P_{l1}, P_{e2}, P_{l2}) + d\sigma(P_{e1}, P_{l1}, -P_{e2}, -P_{l2})}, \quad (1)$$

where $z = \cos\theta$, which are shown in Fig.4. These asymmetries are not only functions of z but are also dependent on the W pair invariant mass M_{WW} in a way that is also sensitive to graviton exchange as shown in the left panel of Fig.5.

By performing a combined fit to the total cross sections and angular distributions, the LL and $LT + TL$ helicity fractions for various initial state polarization choices and the polarization asymmetries we are able to discern the discovery reaches for M_H as a function of the total $\gamma\gamma$ integrated lumi-

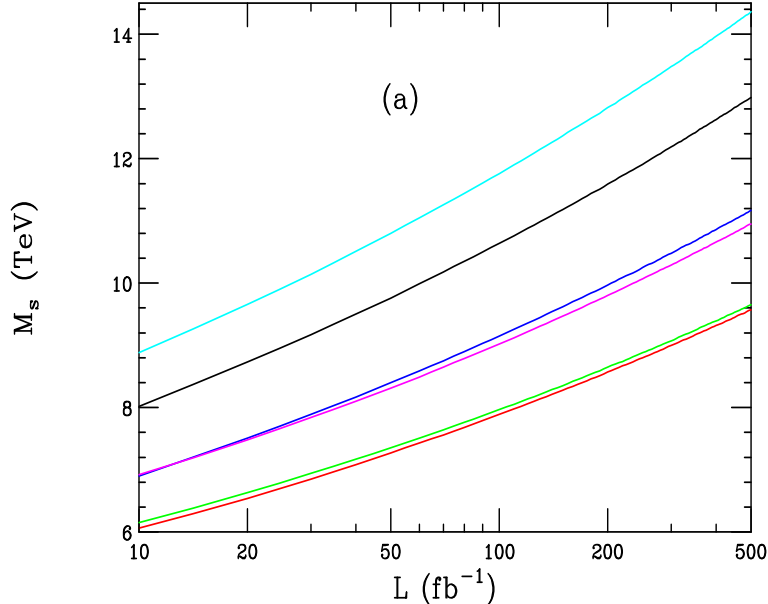


Fig. 6. M_H discovery reach for the process $\gamma\gamma \rightarrow W^+W^-$ at a 1 TeV e^+e^- collider as a function of the integrated luminosity for the different initial state polarizations assuming $\lambda = 1$. From top to bottom on the right hand side of the figure the polarizations are $(- + +-)$, $(+ - --)$, $(+ + --)$, $(+ - +-)$, $(+ - --)$, and $(+ + ++)$.

osity; this is shown in Fig.6. Here we see a search reach in the range of $M_H \sim 11 - 13\sqrt{s}$, which is the larger than that obtained from all other processes examined so far. By comparison, a combined analysis of the processes $e^+e^- \rightarrow f\bar{f}$ with the same integrated luminosity leads to a search reach of $\simeq 6 - 7\sqrt{s}$.

We note in passing that other $\gamma\gamma$ final states are also sensitive to graviton exchange, one example being ZZ final state, which yield smaller search reaches. The right panel of Fig.5 shows the differential cross section due to graviton exchange for this process for different polarization states. These values are significantly larger than those arising from the SM.

4 Conclusion

As can be seen from the discussion above, e^+e^- and $\gamma\gamma$ colliders are quite complementary when it comes to discovering and exploring new physics scenarios. In some cases, such as graviton exchange, the $\gamma\gamma$ reach is superior to that of other colliders.

References

- [1] For a review, see H. Aihara *et al.* in *Electroweak Symmetry Breaking and Beyond the Standard Model*, ed. T. Barklow *et al.*, (World Scientific, Singapore, 1995).
- [2] For a few of the older references, see, for example E. Yehudai, Phys. Rev. **D41**, 33 (1990) and D44 3434 1991 ; S.Y. Choi and F. Schrempp, Phys. Lett. **B272**, 149 (1991); S.J. Brodsky, T.G. Rizzo and I. Schmidt, Phys. Rev. **D52**, 4929 (1995); M. Baillargeon, G. Belanger and F. Boudjema, Nucl. Phys. **B500**, 224, (1997).
- [3] For a review, see A. Djoudai, J. Ng and T.G. Rizzo in *Electroweak Symmetry Breaking and Beyond the Standard Model*, ed. T. Barklow *et al.*, (World Scientific, Singapore, 1995); W. Buchmüller, R. Rückl and D. Wyler, Phys. Lett. **B191**, 442 (1987); J.L. Hewett and T.G. Rizzo, Phys. Rep. **183**, 193 (1989) and Phys. Rev. **D56**, 5709 (1997); J. Blümlein and R. Rückl, Phys. Lett. **B304**, 337 (1993); S. Davidson, D. Bailey, and B.A. Campbell, Z. Phys. **C61**, 613 (1994); M. Leurer, Phys. Rev. **D50**, 536 (1994), and **D49**, 333 (1994).
- [4] A.F. Zarnecki, these proceedings.
- [5] G. Belanger, D. London and H. Nadeau, Phys. Rev. **D49**, 3140 (1994).
- [6] For a review see the first paper in Ref. 3.
- [7] N. Arkani-Hamed, S. Dimopoulos and G. Dvali, Phys. Lett. **B429**, 263 (1998) and Phys. Rev. **D59**, 086004 (1999); I. Antoniadis, N. Arkani-Hamed, S. Dimopoulos and G. Dvali, Phys. Lett. **B436**, 257 (1998).
- [8] G.F. Giudice, R. Rattazzi and J.D. Wells, Nucl. Phys. **B544**, 3 (1999); T. Han, J.D. Lykken and R. Zhang, Phys. Rev. **D59**, 105006 (1999), E.A. Mirabelli, M. Perelstein and M.E. Peskin, Phys. Rev. Lett. **82**, 2236 (1999); J.L. Hewett, Phys. Rev. Lett. **82**, 4765 (1999); for a review see T.G. Rizzo, hep-ph/9910255.
- [9] T.G. Rizzo, Phys. Rev. **D60**, 115010 (1999).